## N: 10.1039/b201424

## Plugged hexagonal templated silica: a unique micro- and mesoporous composite material with internal silica nanocapsules<sup>†</sup>

P. Van Der Voort,\*\*a P. I. Ravikovitch,\*b K. P. De Jong,\*c A. V. Neimark,\*b A. H. Janssen,\*c M. Benjelloun,\*a E. Van Bavel,\*a P. Cool,\*a B. M. Weckhuysen\*c and E. F. Vansant\*a

- <sup>a</sup> University of Antwerp (UIA), Dept. of Chemistry, Universiteitsplein 1, B-2610 Wilrijk, Belgium. E-mail: pascal.vandervoort@ua.ac.be
- <sup>b</sup> Centre for Modelling and Characterisation of Nanoporous Materials, TRI Princeton, P.O. Box 625, Princeton, NJ 08542, USA
- <sup>c</sup> University of Utrecht, Dept. of Inorganic Chemistry and Catalysis, Debye Institute, Sorbonnelaan 16, 3508, The Netherlands

Received (in Cambridge, UK) 8th February 2002, Accepted 25th March 2002 First published as an Advance Article on the web 8th April 2002

We describe in this paper the development of plugged hexagonal templated silicas (PHTS) which are hexagonally ordered materials, with internal microporous silica nanocapsules; they have a combined micro- and mesoporosity and a tuneable amount of both open and encapsulated mesopores and are much more stable than other tested micellar templated structures.

Researchers of Mobil published in 1992 a breakthrough report on the synthesis of ordered mesoporous silica materials. The publication of these results has stimulated a large and worldwide effort to synthesise new types of ordered mesoporous materials.

Due to their controlled pore size and a very narrow pore size distribution, the ordered mesoporous materials have a large potential as catalytic supports in fine chemistry, pharmaceutical industry, as well as for the production of special polymer materials.3 Unfortunately, the actual use of the materials has been severely hampered by their poor stability. Moreover, materials with combined micro- and mesoporosity will offer significant supplementary advantages (improved diffusion rate, multifunctionality, encapsulation capabilities, controlled release rates of an active component, etc.). SBA-15, developed by Stucky and Zhao and their coworkers<sup>2</sup> is a material that has the benefits of a combined micro- and mesoporosity and relatively thick silica walls. Miyazawa and Inagaki4 have recently further improved the synthesis of SBA-15, in order to optimise the ratio micro/meso pores. This procedure yields materials with an increased micropore volume (0.2 cm<sup>3</sup> g<sup>-1</sup>), at the expense however of the total pore volume and surface area (typically 450  $m^2$   $g^{-1}$ ). Here we describe the fast and easy synthesis of stable composite materials, with combined micro- and mesoporosity and large pore volumes. The high micropore volume and high stability of these PHTS materials is governed by internal silica nanocapsules. The experimental part is described in the footnote‡.

All synthesised materials exhibit the typical X-Ray diffraction patterns of the 2D hexagonal pore ordering in the p6mm space group.<sup>2†</sup> The 77 K nitrogen isotherm in Fig. 1 is typical for the newly developed PHTS materials. The following characteristic features can be deducted: (1) adsorption in intrawall micropores at low relative pressures; (2) multilayer adsorption in regular mesopores and capillary condensation, indicating uniform mesopores; (4) a two-step desorption branch indicating the pore blocking effects (sub-step at the relative pressure of ca. 0.45). The adsorption–desorption behaviour is consistent with a structure comprising both open

and blocked cylindrical mesopores. The high pressure desorption step corresponds to nitrogen desorption from open pores. The blocked pores will remain filled until the vapour pressure is lowered to  $p/p_0=0.45$ , after which a cavitation of the condensed  $N_2$  occurs, and closed sections spontaneously empty. This interpretation is supported by the non-local density functional theory (NLDFT) of adsorption and hysteresis in cylindrical pores. Particularly, the shape and width of the hysteresis loop between the capillary condensation and the high pressure desorption step corresponds to the theoretical predictions for cylindrical pores. The mesopore size distribution and the total amount of micropores are calculated from the adsorption branch of the isotherm by the NLDFT method. The fractions of open and closed mesopores have been determined from the pore size distributions (Table 1).

High resolution TEM measurements confirm this model.§

The rather thick walls (~4 nm) of the large cylindrical mesopores are perforated with micropores. Moreover, the cylindrical mesopores themselves are 'plugged' with amorphous silica nanocapsules, which are also microporous. These nanocapsules are created by the large excess of the silica source (TEOS) that is used in the synthesis and by rapid hydrolysis of the silicon alkoxide at the very low pH used. The micropores in the silica walls can be explained by the penetration of hydrophilic poly(ethyleneoxide) chains of the triblock copolymer in the silica wall, as already suggested by Kruk *et al.*<sup>7</sup> The microporosity of the plugs may have a different origin. It is known that Pluronic triblock copolymers are in fact polydisperse mixtures of several triblock copolymers with a wide range of molecular weights, and that they contain appreciable amounts of diblock copolymers and even free PO chains. Some

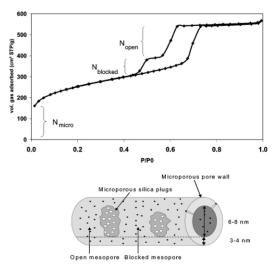


Fig. 1 Nitrogen 77 K isotherm of a typical PHTS material.

<sup>†</sup> Electronic supplementary information (ESI) available: Fig. S1: X-ray diffractogram of a PHTS material. Fig. S2: TEM images of SBA-15 and PHTS-2. Fig. S3: hydrothermal stabilities. See http://www.rsc.org/suppdata/cc/b2/b201424f/

Table 1 Structural characteristics of selected PHTS samples<sup>a</sup>

| Sample | TEOS/P123 | Ageing temp./K | a <sub>0</sub> /nm | $V_{\rm tot}/{\rm cm}^3$ | $S_{\text{BET}}/\text{m}^2$<br>$g^{-1}$ | $V_{ m mi}/{ m cm}^3$ ${ m g}^{-1}$ | $V_{ m me}/{ m cm}^3$ ${ m g}^{-1}$ | $D_{ m pore}$ /nm | h <sub>w</sub> /nm | $V_{ m me,open}/$ cm <sup>3</sup> g <sup>-1</sup> | $V_{ m me,blocked}/$ cm <sup>3</sup> g <sup>-1</sup> | $V_{ m micro}$ (% | V <sub>me,open</sub> ) (%) |
|--------|-----------|----------------|--------------------|--------------------------|---|-------------------------------------|-------------------------------------|-------------------|--------------------|---|--|-------------------|----------------------------|
| SBA-15 | 59        | 353            | 9.70               | 0.70                     | 660                                     | 0.16                                | 0.54                                | 7.00              | 2.70               | 0.54  | 0  | 23                | 100                        |
| PHTS-1 | 84        | 353            | 11.08              | 1.03                     | 1040                                    | 0.29                                | 0.74                                | 6.79              | 4.30               | 0.23  | 0.51   | 28                | 31                         |
| PHTS-2 | 125       | 353            | 10.75              | 0.82                     | 893                                     | 0.30                                | 0.52                                | 6.80              | 3.95               | 0.38  | 0.15   | 36                | 72                         |
| PTHS-3 | 146       | 353            | 9.29               | 0.44                     | 580                                     | 0.17                                | 0.27                                | 5.68              | 3.62               | < 0.01  | 0.27   | 39                | 0                          |
| PHTS-4 | 125       | 373            | 9.52               | 0.66                     | 779                                     | 0.25                                | 0.41                                | 7.00              | 2.52               | 0.08  | 0.33   | 38                | 19                         |

 $<sup>^</sup>a$  Structural characteristics of four selected PHTS samples, synthesised as described in footnote‡ using the indicated TEOS/P123 ratio and ageing temperature.  $a_0$  = lattice spacing,  $V_{\text{tot}}$  = total pore volume (micropores and mesopores),  $V_{\text{mi}}$  = micropore volume,  $V_{\text{me}}$  = mesopore volume,  $D_{\text{pore}}$  = pore diameter from the adsorption branch,  $h_{\text{w}}$  = pore wall thickness,  $h_{\text{w}}$  =  $a_0 - D_{\text{pore}}$ ,  $V_{\text{me,open}}$  = volume of open mesopores,  $V_{\text{me, blocked}}$  = volume of blocked mesopores,  $V_{\text{micro}}$  (%) = percentage of micropores to total pore volume,  $V_{\text{me,open}}$  (%) = percentage of open mesopores to total mesopores.

of these components, especially the low molecular weight ones, may not be involved in the actual templating of the mesopores, but still act as templates for the disordered nanocapsules, inducing a complementary porosity.

Table 1 shows the characteristics of a very limited number of synthesised samples. The thickness of the mesoporous walls is typically 3-4 nm. Very high total pore volumes (up to 1 cm<sup>3</sup>  $g^{-1}$ ) and micropore volumes (up to 0.3 cm<sup>3</sup> g<sup>-1</sup>) can be obtained. Especially the contribution of micropores (with contributions of both micropores in the walls and micropores in the silica nanocapsules) has an unprecedented high value. Both the ratio micropore/mesopore volumes as the ratio open/closed mesopores are tuneable in a wide range. Comparison of samples PHTS-(1-3) shows the important effect of the surfactant/TEOS ratio on the sample characteristics. With increasing TEOS concentrations, the surface area and total pore volume gradually decrease, and also the pore diameter decreases systematically. The amount of 'open' mesopores is variable from 100% for a regular SBA-15 to 0% for PHTS-3. PHTS-4 is to be compared with PHTS-2 and shows the effect of an elevation of the ageing temperature from 353 to 373 K. The average pore diameter is enlarged and the wall thickness decreases from 3.9 to 2.5 nm. These effects are also observable for regular SBA-15 and are explained by the increasing hydrophobicity of the ethyleneoxide chains at higher temperatures.<sup>2</sup>

The thermal, hydrothermal and mechanical stability of the PHTS materials is excellent. Fig. 2 shows the mechanical stability of the most common mesoporous templated materials. The maximum pressure that a material could withstand was defined as the pressure at which the material lost either more than 50% of its pore volume or 50% of the most intensive

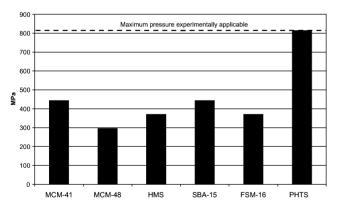


Fig. 2 Mechanical stability of most common mesoporous templated materials.

diffraction band after applying that pressure for 5 minutes. It is obvious from this plot that all conventional materials are relatively unstable towards unilateral pressure. The PHTS material on the other hand can withstand very high pressures. The maximum pressure indicated in the plot is the maximum pressure that could be achieved by our experimental set-up. Also the hydrothermal stability of these materials has been compared. These tests have shown that PHTS (and to a lesser extent SBA-15) are the only materials of the test series that can withstand severe hydrothermal treatments. PHTS can resist a steaming procedure, being placed on a grid above water in an autoclave at 393 K at autogeneous pressure for 24 h. All other materials (MCM-41, MCM-48, HMS, FSM-16) collapse during this treatment.

In conclusion, a new type of porous templated material has been synthesised in a very simple and fast way. The material consists of mesoporous cylinders, consisting of microporous walls. Moreover, microporous silica nanocapsules are present inside the cylindrical mesopores. The structure is fully confirmed by nitrogen adsorption and the NLDFT theory, TEM and XRD. The micropore volume of these structures and their stability are unprecedented.

## Notes and references

- $\ddagger$  Materials were prepared by dissolving Pluronic P123 (non-ionic triblock copolymer, P123, EO<sub>20</sub>PO<sub>70</sub>EO<sub>20</sub>) and TEOS (Si(OC<sub>2</sub>H<sub>5</sub>)<sub>4</sub> in various ratios (cf. Table 1) in a 2 M HCl solution. The solution was stirred for 4–8 h at room temperature, and then aged for 16 h at various temperatures. The white solid was filtered off, washed and calcined at 823 K.
- § The mesopores in SBA-15 run smoothly over several micrometers of length, the PHTS displays smaller domain sizes for the ordered mesopores. Moreover, the silica nanocapsules are clearly visible (see ESI†)
- C. T. Kresge, M. E. Leonowicz, W. J. Roth, J. C. Vartuli and J. S. Beck, Nature, 1992, 359, 710.
- P. T. Tanev, M. Chibwe and T. J. Pinnavaia, *Nature*, 1994, 368, 321; P. T. Tanev and T. J. Pinnavaia, *Science*, 1995, 267, 865; D. Zhao, J. Feng, Q. Huo, N. Melosh, G. H. Fredrickson, B. Chmelka and G. D. Stucky, *Science*, 1998, 279, 548; S. A. Bagshaw, E. Prouzet and T. J. Pinnavaia, *Science*, 1995, 269, 1242.
- A. Corma, *Chem. Rev.*, 1997, **97**, 2373; J. H. Clark, *Green Chem.*, 1999,
   1, 1; B. M. Weckhuysen, R. R. Rao, J. Pelgrims, R. A. Schoonheydt, P. Bodart, G. Debras, O. Collart, P. Van Der Voort and E. F. Vansant, *Chem. Eur. J.*, 2000, **6**, 2960.
- 4 K. Miyazawa and S. Inagaki, Chem. Commun., 2000, 2121.
- 5 A. V. Neimark, P. I. Ravikovitch and A. Vishnyakov, *Phys. Rev. E.*, 2000, 62, R1493.
- 6 P. I. Ravikovitch and A. V. Neimark, J. Phys. Chem. B, 2001, 105, 6817.
- M. Kruk, M. Jaroniec, C. H. Ko and R. Ryoo, *Chem. Mater.*, 2000, 12,
   19.